Geophysical Inversion: Fundamentals and Applications in Mineral Exploration Problems

Oldenburg, D.W.[1], Li, Y.[1], and Farquharson, C.G.[1]

1. Geophysical Inversion Facility, Department of Earth & Ocean Sciences, University of British Columbia, Vancouver, B.C.

ABSTRACT

The nonuniqueness of geophysical inverse problems is well understood and it is now common to solve the inverse problem by minimizing a model objective function subject to a requirement that the data are adequately reproduced. The two main impediments to successful inversion are therefore specifying the objective function to be minimized and how well to fit the data. We outline a general inversion methodology that can be used to invert geophysical data to recover 1-D, 2-D, and 3-D earth models. We focus upon the importance of the objective function and show that attempting to find minimum structure models is a good strategy for a first inversion. Field examples include: TEM data in a tropical environment, DC resistivity and IP data from the Century deposit, magnetic data from Raglan, and gravity data from Voisey's Bay.

INTRODUCTION

In a typical inverse problem we are provided with data d^{obs}, some estimate of their errors, and a relationship $d = \mathcal{F}[m]$ which lets us calculate predicted data that correspond to a model m. Our goal is to find the m which gave rise to the observations. The principal difficulty is nonuniqueness. The observations provide only a finite number of constraints on m and if there is one model that acceptably fits the data there are assuredly many more. An inversion algorithm can generate a model which fits the data but a fundamental question is: "Which one should it construct?" The constructed model should have "character" that emulates the local geology, should fit the geophysical data, and be interpretable. This goal can be achieved by designing an "appropriate" model objective functional $\psi_m(m)$ and finding the m which minimizes that quantity subject to the data constraints. Since geologic environments differ, however, we need a generic objective function which is simple in the number of free parameters it entails, and is yet flexible enough to generate models with different character. Our choice is

$$\psi_m(m,m_0) = \alpha_s \int_{vol} w_s(m-m_0)^2\,dv + \alpha_x \int_{vol} w_x\left(\frac{\partial m}{\partial x}\right)^2 dv + \alpha_y \int_{vol} w_y\left(\frac{\partial m}{\partial y}\right)^2 dv + \alpha_z \int_{vol} w_z\left(\frac{\partial m}{\partial z}\right)^2 dv \qquad [1]$$

In Equation [1] the constant α_s controls the importance of closeness of the constructed model to the base model m_0, and constants α_x, α_y, α_z control the roughness of the model in the horizontal and vertical directions. These are global control quantities. More specific control on the structure can be achieved by adjusting the functions w_s, w_x, w_y, w_z but, as a first pass, these are generally set to unity. Equation [1] provides the needed practical flexibility to generate a variety of models. By altering the parameters the user can incorporate additional information into the inversion, generate a preferred model, carry out hypothesis testing regarding the existence of particular structures seen in the inverted image, and explore non-uniqueness. This flexibility of course means that any geophysical data set will be inverted a number of times and thus the algorithm needs to be computationally efficient.

To solve the problem numerically we divide our model into M rectangular cells and assume the physical property is constant within each cell. The cells should be sufficiently small so that discretization does not affect the final solution. This makes our formalism different from parametric approaches to solving the inverse problem. The "model" for the inverse problem becomes an M-length vector $\vec{m} = (m_0, m_1, \ldots m_M)$. The objective function can be written as $\psi_m(\vec{m})$ and our goal is to minimize this subject to data constraints. Unfortunately the data are not accurate and this raises the next important question "What are the errors in the data?" or relatedly, "How well should the data be reproduced?" Different measures of misfit are possible. We use a misfit criterion $\psi_d = \left\| W_d(\vec{d} - \vec{d}^{obs}) \right\|$ where W_d is a data weighting matrix whose elements are usually reciprocals of estimated standard deviations of the data. With the assumption of Gaussian noise, the misfit has an expected value, and our problem is solved by minimizing ψ_m subject to $\psi_d = \psi_d^*$, where ψ_d^* is a target misfit. The solution is straight forward if the relationship between the model parameters and data is linear.

In "Proceedings of Exploration 97: Fourth Decennial International Conference on Mineral Exploration" *edited by* A.G. Gubins, 1997, p. 545–548

However, because of the uncertainty in knowing the true errors, the recovered model may be deemed to be too rough or too smooth. This requires a subsequent inversion with a different target misfit.

In the more usual case where the relationship between model and data is nonlinear then iterative procedures must be used to solve the inverse problem. One begins with a starting model $\vec{m}^{(0)}$ and at each iteration a perturbation $\partial\vec{m}$ is calculated to update the model. Sensitivities $J_{ij} = \partial d_i / \partial m_j$, which quantify how the *i'th* datum is altered when the *j'th* model parameter is changed, are required. The solution for $\partial\vec{m}$ is obtained by solving an $M \times M$ system of equations.

APPLICATIONS TO FIELD DATA

The work presented in this paper has been completed under the JACI research consortium which is an acronym for "Joint and Cooperative Inversion of Geophysical and Geological Data." Throughout the research a number of algorithms have been developed and made available to the sponsors. The following mini-case histories have been provided by the sponsors and they illustrate our inversion methodology in 1-D, 2-D and 3-D.

1-D Inversion of TEM Data

As an example of 1-D inversion we invert time domain electromagnetic (TEM) data in a tropical environment. The goal was to determine the thickness of a relatively conductive saprolitic overburden layer. A Geonics Protem 47 transmitter attached to an 8-turn 5×5 metre square loop provided the source, and the receiver was a high-frequency coil system. Data were recorded 20 m from the loop and the station interval was 25 m. The ramp time for the transmitter was 10 μsec and 20 time channels of data were recorded. 5000 soundings were acquired. The data were transmitted by satellite to Placer Dome in Vancouver, inverted, and the interpreted conductivity models returned to the field by fax. The 1-D inversion algorithm of Farquharson & Oldenburg (1993) was used to invert each sounding and the models were concatenated into 2-D sections. In carrying out the inversion the earth model was divided into 30 layers of successively increasing thickness and $m_i = log\,\sigma_i$ was used as the model parameter. The objective function was designed to penalize structure in the vertical direction. This was accomplished by setting α_s, α_x, α_y equal to zero in Equation [1]. The problem is nonlinear and solved iteratively. Gaussian errors varying from 1% for the earliest time channel to 20% for the latest time channel were assigned to the data.

The recovered resistivities from four lines, separated by 200 m, are shown in Figure 1. The purely white areas coincide with locations where data acquisition was not possible because of surface ponds of water. The objective function in the inversion penalizes variation of conductivity in the vertical direction and hence existing layer boundaries will be observed as transition zones. For this example the large contrast between the saprolite and the resistive bedrock shows up as a reasonably well defined boundary. Overall, the overburden layer has been reasonably well defined and its variability and depth have been verified in subsequent drilling.

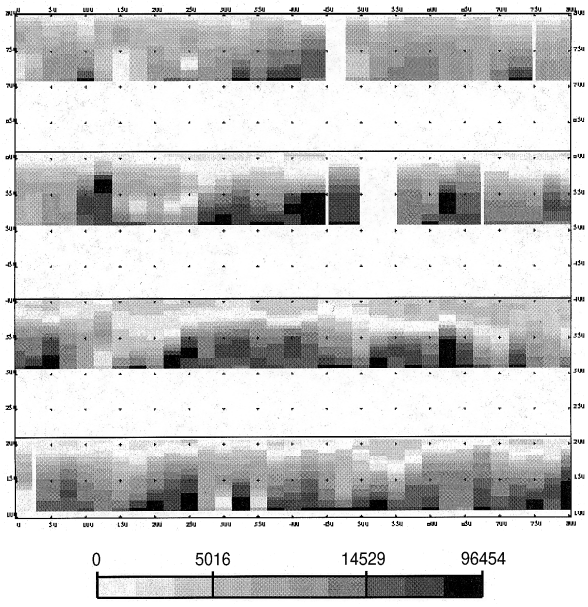

Figure 1: *Resistivity models recovered from 1-D inversion of TEM data along four adjacent traverses. The series of 1-D models are "stitched" together to form a 2-D section along each line. The grayscale indicates the resistivity in Ωm. The conductive zones near the surface exhibit reasonable continuity along each line and from line to line.*

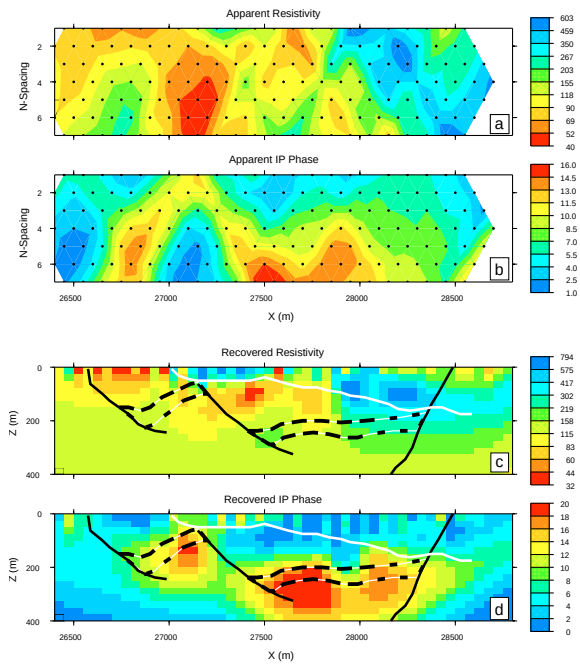

Figure 2: *DC and IP inversion of Line 47000E at Century deposit. Panels (**a**) and (**b**) are the apparent resistivity and apparent IP phase pseudo-sections, respectively. The grayscales indicate the resistivity in Ωm and phase in mrad. Panels (**c**) and (**d**) are the inverted resistivity and phase sections, respectively. Overlaid on the sections are the boundary of the overburden (white line), three faults (black lines), and the boundaries of the orebody (dashed lines).*

2-D inversion of DC resistivity and IP data

In 2-D problems the model varies in the x and z directions and, correspondingly, the first three terms of the objective function in Eq [1] are needed. Again the model discretization should be small enough that the parameterization does not have any affect of the inverted result. For DC resistivity and IP data this typically means solving a problem with a few thousand cells and a few hundred data.

The Century deposit is located approximately 250 km NNW of Mt. Isa in NW Queensland Australia and is hosted by relatively flat lying middle Proterozoic siltstone and shale units. Mineralization occurs preferentially within black shale units as fine grained sphalerite and galena with minor pyrite. Complex resistivity dipole-dipole data with α=100, n=1,7 were collected over the deposit and inverted by CRA Exploration Pty Ltd. Apparent resistivity and IP pseudo-sections for the line 47000E are shown in Figures 2a and 2b. The 177 data are inverted using the algorithm described in Oldenburg and Li (1994). The earth is divided into 2000 rectangular cells each having a constant resistivity and chargeability. First the DC resistivity data are inverted. Data are assigned a 3% error and the coefficients $(\alpha_s, \alpha_x, \alpha_z)$=(.001, 1, 1) generate a model that is equally smooth in horizontal and vertical directions and has a tendency to return to the base model of 10 Ωm at depth where the data no longer constrain the model. The inversion is nonlinear and iterations are required. The variable for the inversion is $\log\rho$. The recovered model is shown in Figure 2c along with a superposed geologic section. The inversion nicely delineates the resistive overburden on the right hand side, but the resistivity is not correlated with mineralization.

The resistivity model in Figure 2c is used to calculate the sensitivity matrix for inversion of the IP data. The model discretization for IP inversion is the same as for DC resistivity. The reference model is zero and data are ascribed an error of 0.5 mrad. The chargeability model with geologic overlay is shown in Figure 2d. The IP inversion has delineated the horizontal extent and depth to the orebody. It also indicates a major fault between x=27,000 m and x=27,500 m which dislocates the ore sequence. The chargeable body on the inverted section is somewhat thicker than drill hole results. This occurs for two reasons. Our objective function constructs smooth models, and hence discrete boundaries will appear as gradational images. Also, downhole IP and petrophysical data indicate that while Century ore is strongly polarisable, the adjacent units, particularly the footwall sediments, are weakly chargeable. This adds to the response and thickens the region of polarization. Overall, the IP image provides important information about both mineralization and structure.

3-D inversion of magnetic data

In 3-D problems all components of the objective function in Equation [1] are required. The number of data are typically about a thousand, and the number of cells is a few tens of thousand. For the magnetic inversion we neglect remanent magnetism and self-demagnetization effects but require that the susceptibility be positive. The procedure outlined in Li and Oldenburg (1996) is used. A crucial aspect of their inversion is the incorporation of a depth weighting of the form $w(z) = 1/(z+z_0)^3$ into all components in the objective function. This counteracts the natural $1/r^3$ decay of the kernels and allows the program to distribute the susceptibility in depth. In the depth weighting, z_0 depends upon the observation height and cell size and is straightforwardly calculated.

Total field magnetic data taken over the Raglan Deposit are shown in Figure 3. Two regions of high magnetic field are observed. These coexist with ultramafic outcrops and the geologic question was whether the outcrops were associated with a single flow unit. For the 3-D inversion the earth was modelled with a $40\times40\times10$ grid of cells (16,000 cells) and the horizontal dimensions of the cells was 100 × 100 m. The data were assumed to have noise of 2% plus 5 nT. In defining the objective function we set $\alpha_s = 0.0001$, $\alpha_x = \alpha_y = \alpha_z = 1$ and the reference model equal to zero. Positivity was included in the inversion. The recovered model, provided by Falconbridge, was obtained after 25 iterations. Almost all of the misfit occurs at the outcrops. The 100×100 m cells are simply too large to handle the extreme variability of the near-surface magnetic susceptibility. However, the data outside these outcrops is adequately reproduced.

An important aspect of 3-D inversion is the ability to display a 3-D model. A 3-D cube of susceptibilities can be displayed in cross-sectional cuts or as a 3-D-isometric image after volume rendering. Cross-sectional cuts have the advantage that values of the physical property in

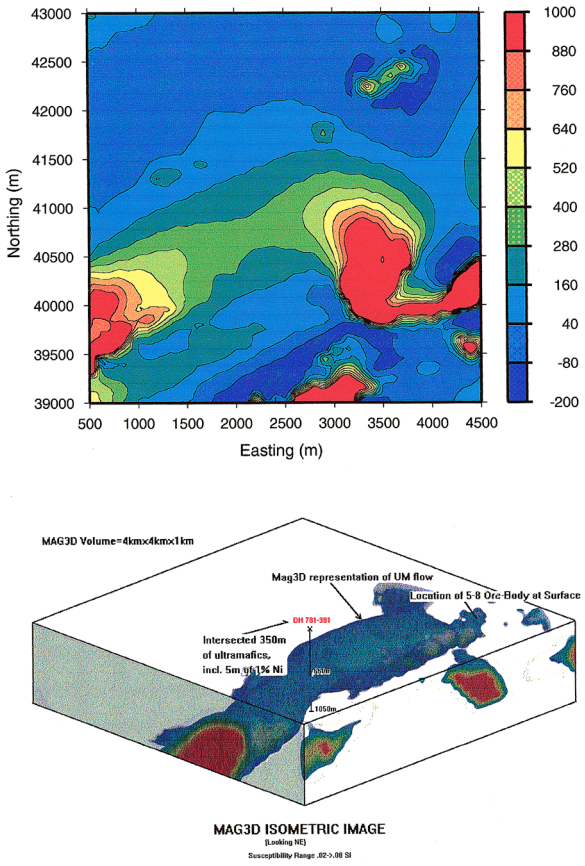

Figure 3: *3-D magnetic inversion at Raglan Deposit. The top panel shows the total field aeromagnetic data. The inducing field has I=83° and D=–32°. The data are contoured in nT on the scale shown by the grayscale bar, but the peak value bear the magnetic high towards the southeast corner exceeds 5 000 nT. The lower panel is a volume rendered image of the inverted susceptibility model, and the displayed surface provides a representation of the ultramafic flow. Indicated in this representation is the intersecting drillhole that was spotted based upon the inversion result.*

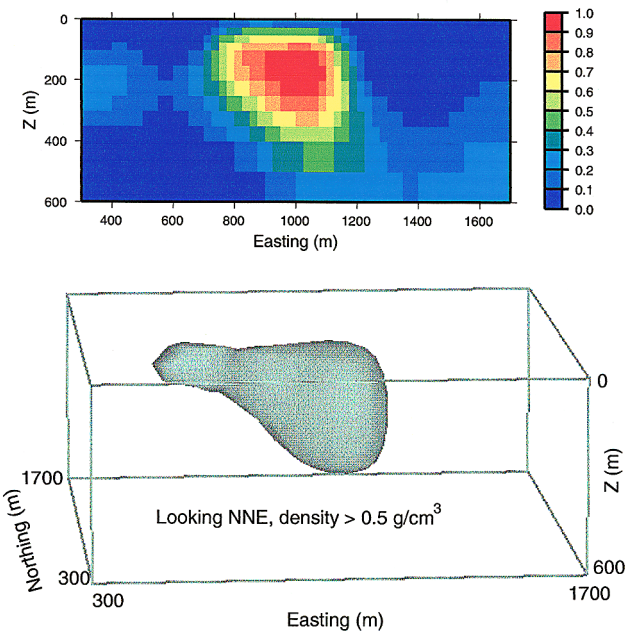

Figure 4: *3-D inversion of gravity data at Voisey's Bay deposit. The top panel shows a cross-section at 1 000m north from the inverted 3-D density model. The grayscale indicates the density in g/cm³. The lower panel shows a volume rendered image of the 3-D density anomaly. The cutoff value is 0.5 g/cm³. This image represents the geometry of the orebody well.*

each cell are displayed. These are the numbers which reproduce the field data and from which quantitative questions can be answered. The disadvantage of the cross-sections is that it is sometimes difficult to get a sense of 3-D structure. This is where 3-D volume rendered images have an advantage, but care must be taken since a different threshold for volume rendering will generate a different image. Here we present the 3-D isometric image generated by Falconbridge. The threshold level is about .04 so susceptibilities less than that are transparent. It was this image that persuaded the project geologist to spot the deep 1100 m hole and provided confidence that the apparently isolated outcrops on the "5–8 Ultramafic Flow" and the "Katinniq flow" to the west were in fact connected at depth. The targeted magnetic source was intersected at 650 m. As a bonus they intersected a 5 m mineralized section (sub-ore grade, approximately 1% Ni) within the 350 m thick intersection of magnetic ultrafmafics.

3-D inversion of gravity data

3-D inversion of gravity data is similar to the 3-D inversion of magnetic data. The primary difference is in the exponent for the depth weighting function. The field from an elementary mass falls off as $1/r^2$ rather than $1/r^3$ as they do in magnetics. Correspondingly the depth weighting is $w(z) = 1/(z+z_0)^2$. The algorithm of Li and Oldenburg (1997) has been applied by INCO on the Voisey's Bay deposit. The earth was modelled as 38 000 cells. The cell dimension varies from 25 m in the central region to 200 m towards the edge. The objective function was defined by using $\alpha_s = 0.0001$, $\alpha_x = \alpha_y = \alpha_z = 1$ and a reference model equal to zero. Positivity was included in the inversion. A total of 1900 Bouguer anomaly data were inverted to recover the density model, and the assumed error was 3% plus 0.01mGal. The inversion converged to the desired misfit. In Figure 4 we show the final model in the central region of the inversion, which encloses the Ovoid orebody. The cross-section at 1,000 m north shows a region of high density at the location of Ovoid orebody, whose thickness increases from the west to the east. The recovered density has a maximum of 1.0 g/cm³ in this section, but it reaches 1.4 g/cm³ in other sections. This is in accordance with the knowledge that the massive sulphide body has a maximum density of 4.5 g/cm³ within a host whose density is 2.8 g/cm³. Since the density model is obtained from a smooth inversion, depending upon the criterion used, the exact position of the boundary can vary. Nevertheless, INCO had estimated a depth to the top of 30 m, while the true overburden thickness varies between 10m and 20 m. The bottom panel in Figure 4 is a volume rendered image of the 3-D density model with a cutoff value of 0.5 g/cm³. This image provides a good representation of the geometry of the orebody.

CONCLUSION

In this paper we have presented a single methodology which can be used to invert geophysical data to recover 1-D, 2-D or 3-D distributions of an appropriate physical property. The two greatest problems in implementing the geophysical inversions are: (1) specifying the model objective function to be minimized and (2) specifying the misfit functional and deciding how well to fit the data. When careful attention is paid to these aspects, it is possible for the inversion algorithm to provide meaningful and valuable information about the earth. The field examples presented here validate this comment and hopefully they are a motivating force to ensure that all geophysical data are ultimately inverted.

ACKNOWLEDGEMENTS

This work was supported by an NSERC IOR grant and an industry consortium "Joint and Cooperative Inversion of Geophysical and Geological Data." Participating companies are Placer Dome, BHP Minerals, Noranda Exploration, Cominco Exploration, Falconbridge, INCO Exploration & Technical Services, Hudson Bay Exploration and Development, Kennecott Exploration Company, Newmont Gold Company, Western Mining Corporation, and CRA Exploration Pty. We are especially grateful to Peter Kowalczyk, Michael Ehling, Bob Smith, Theo Aravanis, Tony Watts, Alan King, and Ping Zhang for supplying data and inversion results for the field examples.

REFERENCES

Farquharson, C.G. and Oldenburg, D.W., 1993, Inversion of time-domain electromagnetic data for a horizontally layered Earth, Geophysical Journal International, **114**, 433-442.

Li, Y. and Oldenburg, D.W., 1996, 3-D inversion of magnetic data, Geophysics, **61**, 394-408.

Li, Y. and Oldenburg, D.W., 1997, 3-D inversion of gravity data, Geophysics (accepted).

Oldenburg, D.W. and Li, Y., 1994, Inversion of induced polarization data, Geophysics, **59**, 1327-1341.